Magnetization modes modelling and analysis for controlled reactors with a rotating field

IOP Conf. Series: Materials Science and Engineering **675** (2019) 012049 doi:10.1088/1757-899X/675/1/012049

Magnetization modes modelling and analysis for controlled reactors with a rotating field

E I Zabudskiy* and G I Balandina

Peoples' Friendship University of Russia (RUDN University), Moscow, Russia

E-mail: zabudskiy-ei@rudn.ru

Abstract. Electromagnetic reactors are used to carry out practical tasks of automatic control of power lines operation modes, distribution grids and energy supply systems of the industrial enterprises. The reactors' characteristics significantly depend on the harmonic's manifestation magnetic field saturation, which is different in the magnetization modes of reactors: forced, free and symmetrical. For the purpose of their analysis, a generalized mathematical model of the cross-sectional magnetic circuits of static ferromagnetic devices with rotating magnetic field has been developed on the base of nonlinear magnetic circuits theories. It was found that the best mode is symmetric magnetization, characterized by the following advantages: an increased range of reactive power control, enhanced stabilizing effect on the controlled current, reduced losses in steel, increased speed and the absence of "shaking" vibrations of the reactor magnetic core. It is shown that the free magnetization mode is close in its merits to the symmetric magnetization mode.

1. Introduction

In the second decade of the twentieth century, the outlines of one of the problems of high-voltage power transmission technology were outlined, consisting in the fact that at large distances the capacitive conductivity of the line starts to have a significant effect and the capacitive current significantly decreases, which reduces the line capacity. This phenomenon was accompanied by an unacceptable increase in voltage.

In the early 40-ies of XX century R. Rüdenberg (Germany) proposed to solve this problem using a strong magnetic saturation of electrical steel, pointing to the need to eliminate the higher harmonic. R. Rüdenberg's ideas were developed in the works of E. Friedlander (GEC, England). GEC company has manufactured and installed more than 50 ferromagnetic reactors at power from tens to hundreds of Mvar in various countries [1-3].

In Russia, a group of organizations led by M.A. Bryantsev mastered the production of a series of high-voltage controllable reactor 25, 32, 63, 100, 180 MV·A for the 500 kV grids. The series of arc-quenching magnetically controlled reactors with oil cooling with a capacity from 190 to 1520 kV·A and a voltage 6-10 kV were developed and massively introduced [4-6].

As a means of regulating reactive power, reactors are necessary to control the modes of electric power systems in order to solve problems: compensation of excess charging power of power lines (transmission lines) and increase their capacity, limit switching overvoltages and short-circuit currents, reduce voltage fluctuations, rational distribution of voltage and current, etc [7-9].

Controlled reactor (CR) is a static energy nonlinear device, which operation is based on the phenomenon of electromagnetic induction. The active part of the reactor contains one or more windings and a magnetic core. The reactive power it consumes is regulated by changing the saturation of the magnetic circuit. The operating range of magnetic induction values is located behind the "knee" of the magnetization curve.

This is due to the appearance of harmonics of the magnetic field saturation, which affect the characteristics of the reactors.

There are three modes of magnetization, which are determined by the manifestation of these harmonics: the forced magnetization (FM) mode in which harmonics are present in the induction of the magnetic field; the mode of free magnetization by the 2nd harmonic (MH2) in which this harmonics are manifested mainly in the magnetic field strength; the mode of symmetric magnetization (SM) in which, when magnetizing the magnetic circuit, even harmonics are absent in the induction and in the magnetic field strength [3, 8, 10].

The purpose of this research was to analyze the listed magnetization modes, their influence on the properties of the reactors and ascertain the best mode of magnetization, a positive effect on the characteristics of the reactors.

2. Method of research

The process of researching devices should be preceded by the implementation of the model-algorithm-program triad, so the device is replaced with its model, which is then analyzed using PC experimentation using computational logic algorithms.

The mathematical model, based on the theory of nonlinear magnetic circuits, takes into account the discrete structure of the tooth-slot layer, the non-magnetic gap between the stator and rotor, the spatial-temporal spectrum of saturation harmonics, and the MMF values of the reactor windings. The derivation of a mathematical model of the magnetization regimes of reactors in general form is given in [8,3,10]. For the analysis of the free magnetization mode by the 2nd harmonic, the model is presented in the form (1), and for the symmetric magnetization mode – (2). On the basis of the developed generalized mathematical model of the phenomena arising at magnetization of a magnetic circuit, the best modes of magnetization are established.

3. Magnetization modes analysis

3.1. Forced magnetization mode

The forced magnetization (FM) mode under the higher harmonics by the saturation of the magnetic field is considered as a mode in which these harmonics appear in the induction of the magnetic field but are practically absent in the field strength.

In order to explore the influence of the field higher harmonics on the operating modes of a controllable reactor (CR), the graphs, reflected the mutual influence of the main harmonics of a rotating field and a bias field are given. The nature of the change in the amplitudes of higher harmonics of saturation from various factors are also to be deduced. For that, the results of PC calculations of a nonlinear transcendental equation that simulates a magnetic circuit of a reactor operating in various magnetization modes, including the FM mode, are used [8].

Later in the document there are the calculated curves for the reactor, which correspond to rational values of the quantities defined in [6]: the ratio of the transverse geometric dimensions of the magnetic circuit $L_{za}^{*} = 0.22$, $d_a^{*} = 0.6$; the number of pole pairs of the three-phase working winding $p_1 = 1$; the relative magnitude of the nonmagnetic gap $\delta^{*} = 50$.

Dependencies $F_1^{*} = f(F_{0a}^{*})$ at $B_1^{*} = const$, named IO curves, are shown in figure 1. They reflect the relationship between the amplitude of the magnetomotive force (MMF) of the three-phase winding F_1^{*} and MMF of the control winding F_{0a}^{*}, which is practically linear in the working range.

Figure 2 displays the dependence $F_{0a}^{*} = f(\delta^{*})$ at $B_1^{*} = const$ and $F_1^{*} = const$. As can be seen from the graph, with an increase in the gap δ^{*} for the given B_1^{*} и F_1^{*} the MMF value of the control ring winding necessary to ensure a certain level of MMF F_1^{*}, decreases. This is natural, since an increase in the gap in itself leads to an increase in the MMF F_1^{*}. However, it is not advisable to increase the gap in the reactor in order to reduce the F_{0a}^{*} at $F_1^{*} = const$ and $B_1^{*} = const$ or in order to reduce the MMF F_1^{*} at $F_{0a}^{*} = const$ and $B_1^{*} = const$, since this drastically limits adjustment capability of the reactor.

Figure 3*a* shows the curves $B_1^{*} = f(F_1^{*})$ at $F_{0a}^{*} = const$, which should be used in the reactor calculation. It's seen from the figure, that the reactor working inductions should be taken from the part of the magnetization curve within $6 \le B_1^{*} \le 7$. More precise recommendations on the choice of B_1^{*} are given in [3, 8].

The curved $B_1^* = f(F_{0a}^*)$ at $F_1^* = const$, shown in figure 3*b* are conveniently used for the calculation when the reactor is switched on with a load [3].

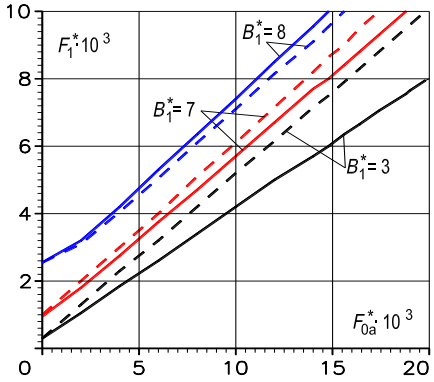

Figure 1. The dependence of the amplitude of the MMF F_1^* on the MMF F_{0a}^* with $\delta^* = 50$, $L_{za}^* = 0.22$, $d_a^* = 0.6$, $p_1 = 1$ in the modes: FM – solid lines and MH2 – dotted.

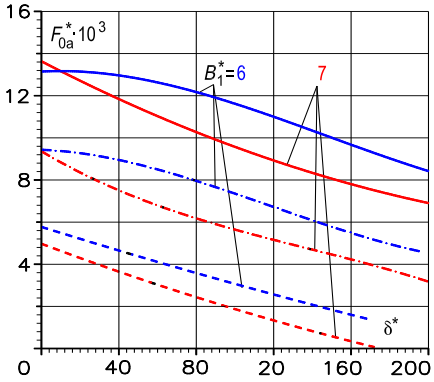

Figure 2. The dependence of the MMF F_{0a}^* on the size of the gap δ^*: the amplitude of the MMF $F_1^* = 7\cdot10^3$ (solid lines); $5\cdot10^3$ (dot-dashed); $3\cdot10^3$ (dotted).

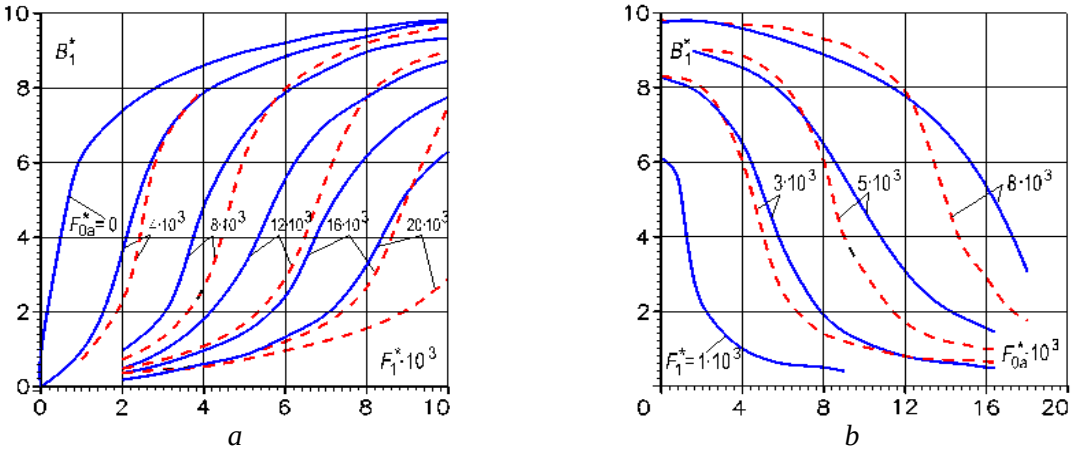

Figure 3. The dependence of the amplitude B_1^* 1st induction harmonic in yokes in the modes: FM – solid lines, MH2 – dotted; *a* – on the amplitude F_1^* of the 1st MMF harmonic at $F_{0a}^* = const$; *b* – on the MMF value F_{0a}^* at $F_1^* = const$.

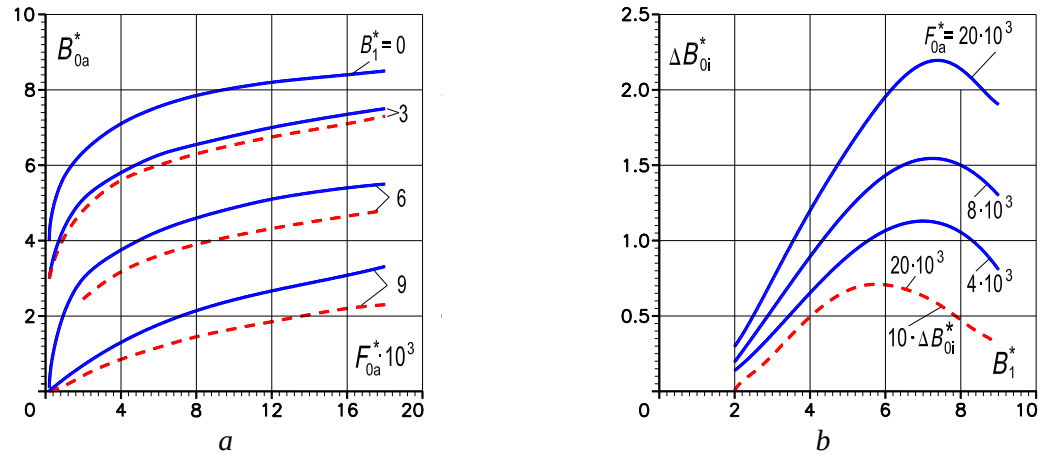

Figure 4. The dependence of the induction value B_{0a}^* on MMF F_{0a}^* at $B_1^* = const$ (*a*) and ΔB_{0i}^* on the amplitude B_1^* at $F_{0a}^* = const$ (*b*) in the modes: FM – solid lines, MH2 – dotted.

The curves, shown on the figure 4, illustrate a decrease in the induction of a constant field with an increase in the amplitude of the main harmonic of induction B_1^* (*a*) and a change in the constant induction component ΔB_{0i}^* in the non-magnetized yoke (*b*) [8].

Next, we find out the dependence of the amplitudes of higher harmonics of saturation on the transverse geometry of the magnetic circuit and other factors.

Figure 5*a,b* shows dependences of the 2nd and 3rd harmonics of induction in the function F_{0a}^* and B_1^* for a reactor with $p_1 = 1, L_{za}^* = 0.22, d_a^* = 0.6$ and $\delta^* = 50$. The second harmonic essentially only grows with increasing bias (figure 5*a*).

With a constant magnetization and variations B_1^* the 2nd harmonic of induction has a maximum at certain values of B_1^* (figure 5*b*), which correspond to the operating inductions of the reactor. At the same time, it does not affect the shape of the controlled current curve, since having the number of pole pairs $2p_1 = 2$, the 2nd harmonic induces in the sides of the coils of a three-phase six-zone 2-pole winding EMF equal in magnitude but opposite in sign. The third harmonic for large values of B_1^*, when the steel is saturated with a rotating field, slightly depends on the degree of bias in the constant field.

The effect on the CR properties of odd harmonics of induction is small, since they have an insignificant value at $B_1^* = 6\ldots7$ and the magnetization of the yokes. In particular, the 3rd harmonic with $B_1^* = 7$ and no bias (idle mode) is $B_3^* = 0.38$, or 5.15% of the first harmonic; at $B_1^* = 7$ and $F_{0a}^* = 8000$ $B_3^* = -0.1$, or 1.43% (figure 5*b*).

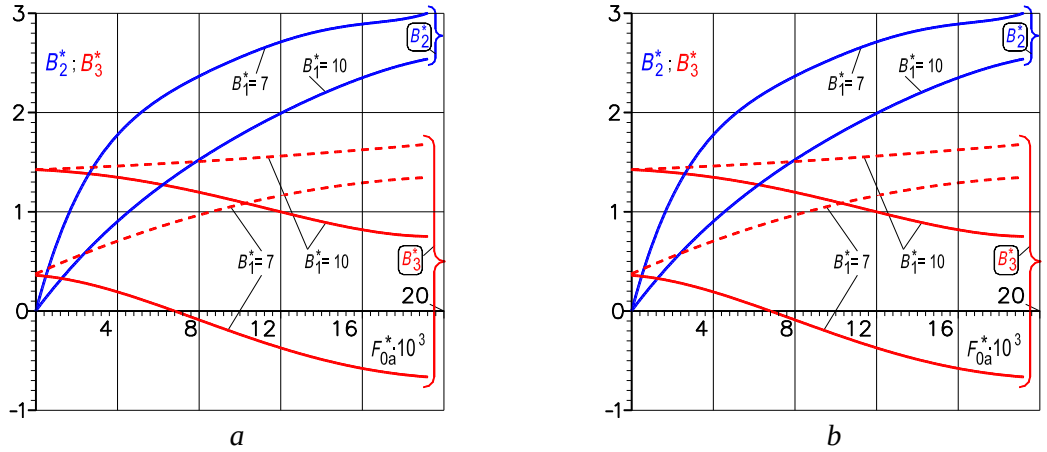

Figure 5. The dependence of the amplitudes of the 2nd and 3rd harmonics in MF modes – solid lines; MH2 – dashed: *a* – on the value of the MMF F_{0a}^*; *b* – from the amplitude of induction B_1^*.

3.2. Free magnetization mode

The free magnetization mode by the higher saturation harmonics is a mode in which these harmonics present in the magnetic field strength, and practically absent in magnetic induction.

The controlled reactor in the unforced magnetization mode at the 2nd harmonic of saturation (UM2) has, in addition to the 2-pole winding and the control winding, also a 4-pole antivibration winding.

In order to determine the characteristics of the reactor in the MH2 mode, the non-linear equation of the magnetic circuit was calculated on a PC [8].

Taking into account the assumptions made in [8] and the reactor design, the nonlinear equation for the mode being analyzed at time $t = 0$ will take the following form:

$$p_1 F_1^* \sin p_1\gamma - 2p_1 F_2^* \cos 2p_1\gamma + \frac{F_{0a}^*}{\pi} + 2\sinh(B_{0a}^* + A_1^*) +$$
$$+2k_s \sinh(\Delta B_{0i}^* + A_1^*) + 2L_{za}^* d_a^* p_1^2 A_2^* \cosh d_a^* p_1 A_3^* + 2\delta^* p_1^2 A_2^* = 0, \quad (1)$$

where A_1^*, A_2^*, A_3^* are respectively expressions

$$A_1^* = -B_1^* \sin p_1\gamma - B_3^* \sin 3p_1\gamma + B_4^* \cos 4p_1\gamma - B_5^* \sin 5p_1\gamma + +B_6^* \cos 6p_1\gamma - B_7^* \sin 7p_1\gamma;$$

$$A_2^* = -B_1^* \sin p_1\gamma - 9B_3^* \sin 3p_1\gamma + 16B_4^* \cos 4p_1\gamma - 25B_5^* \sin 5p_1\gamma + \\ +36B_6^* \cos 6p_1\gamma - 49B_7^* \sin 7p_1\gamma;$$

$$A_3^* = B_1^* \cos p_1\gamma + 3B_3^* \cos 3p_1\gamma + 4B_4^* \sin 4p_1\gamma + 5B_5^* \cos 5p_1\gamma + +6B_6^* \sin 6p_1\gamma + 7B_7^* \cos 7p_1\gamma.$$

There are nine unknowns in the equation: $F_1^*, F_2^*, B_{0a}^*, \Delta B_{0i}^*, B_3^*, B_4^*, B_5^*, B_6^*, B_7^*$.

The calculation was carried out for the rational geometric relations defined in [3] $d_a^* = 0.6$; $L_{za}^* = 0.22$ with the number of pole pairs of the working winding $p_1 = 1$. When calculating the relative length of the gap δ^* is assumed to be 50.

In figure 1, 3 and 4*a* dotted lines (MH2 mode) represent the dependencies:

1) $F_1^* = f(F_{0a}^*)$, $B_1^* = const$; 2) $B_1^* = f(F_1^*)$, $F_{0a}^* = const$;

3) $B_1^* = f(F_{0a}^*)$, $F_1^* = const$; 4) $B_{0a}^* = f(F_{0a}^*)$, $B_1^* = const$.

From figure 1 and 3*a*, it follows that the control range in the MH2 mode with operating inductions $B_1^* = 6\ldots7$ is greater than in the FM mode. To achieve the same value of the MMF F_1^* in MH2 mode, a smaller value of the MMF F_{0a}^* is required than in the FM mode (figure 3*b*). Finally, the $B_{0a}^* = f(F_{0a}^*)$ curves of the analyzed mode are lower than the FM mode curves (figure 4*a*). This is explained by the decrease in the additional constant components of the magnetic induction ΔB_{0a}^* and ΔB_{0i}^*, caused by "magnetic rectification" [8]. Figure 4*b* shows the dependence $\Delta B_{0i}^* = f(B_1^*)$ at $F_{0a}^* = const$. A decrease in the induction constant components in the yokes leads to some reduction in the loss in steel. The third harmonic in the MH2 mode as compared to the FM mode does not change its phase (figure 5).

The graphs of the amplitude change of the MMF of the anti-vibration winding $F_2^* = f(F_{0a}^*)$ at $B_1^* = const$ and $F_2^* = f(B_1^*)$ at $F_{0a}^* = const$, which are used in the design of the reactor, are shown in figure 6. With working inductions $B_1^* = 6\ldots7$ and $F_{0a}^* = 12000$ the MMF value F_2^* is approximately 25% of the MDS of the working winding F_1^*.

Summing up the analysis of the free magnetization mode on the 2nd harmonic, we note that the latter favorably differs from the forced magnetization mode by a significant decrease in the vibrations of the magnetic circuit and an extended range of operating current control, as evidenced experimental data [3].

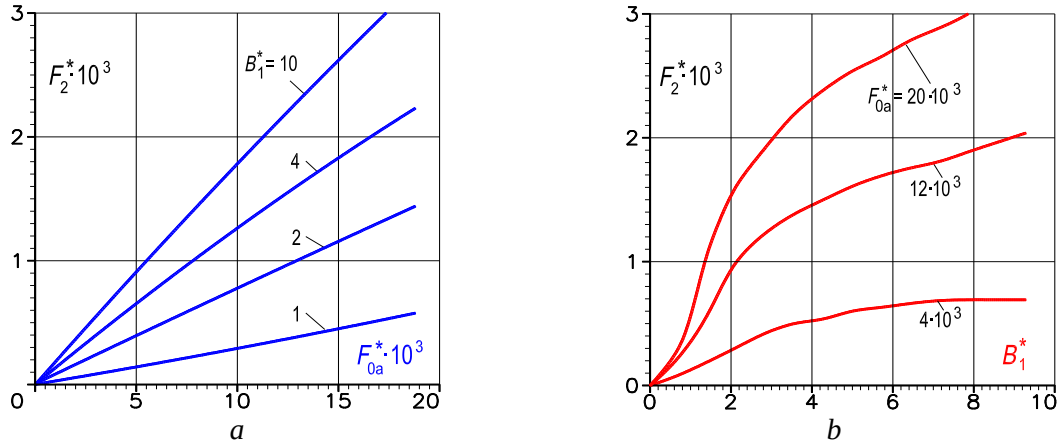

Figure 6. The dependence of the amplitude of the MMF F_2^* in MH2 mode:
a – from the value of the MMF F_{0a}^*; *b* – from the amplitude of induction B_1^*.

3.3. Symmetric magnetization mode

The symmetric magnetization mode (SM) is a mode, in which, with magnetic bias, even saturation harmonics practically do not appear either in induction or in the magnetic field.

For study of the operation of the reactor in the SN mode, we use the results of the calculation of the nonlinear magnetic circuit equation on a PC [8]. Considering the assumptions made in [8] and the reactor design, see (figure 13), this equation for the time t = 0 is written as

$$p_1F_1^* \sin p_1\gamma + \frac{F_{0a}^*}{\pi} + \frac{F_{0i}^*}{\pi} + 2\sinh(B_{0a}^* + A_1^*) + 2k_s \sinh(B_{0i}^* + A_1^*) + \\ +2L_{za}^* d_a^* p_1^2 A_2^* \cosh d_a^* p_1 A_3^* + 2L_{zi}^* d_i^* p_1^2 A_2^* \cosh d_i^* p_1 A_3^* + 2\delta^* p_1^2 A_2^* = 0, \qquad (2)$$

where A_1^*, A_2^*, A_3^* are respectively expressions

$$A_1^* = -B_1^* \sin p_1\gamma + B_2^* \cos 2p_1\gamma - B_3^* \sin 3p_1\gamma + B_4^* \cos 4p_1\gamma - B_5^* \sin 5p_1\gamma + \\ +B_6^* \cos 6p_1\gamma - B_7^* \sin 7p_1\gamma;$$

$$A_2^* = -B_1^* \sin p_1\gamma + 4B_2^* \cos 2p_1\gamma - 9B_3^* \sin 3p_1\gamma + +16B_4^* \cos 4p_1\gamma - 25B_5^* \sin 5p_1\gamma + \\ +36B_6^* \cos 6p_1\gamma - 49B_7^* \sin 7p_1\gamma;$$

$$A_3^* = B_1^* \cos p_1\gamma + 2B_4^* \sin 2p_1\gamma + +3B_3^* \cos 3p_1\gamma + 4B_4^* \sin 4p_1\gamma + 5B_5^* \cos 5p_1\gamma + \\ +6B_6^* \sin 6p_1\gamma + 7B_7^* \cos 7p_1\gamma.$$

There are nine unknowns in the equation (2): $F_1^*, B_{0a}^*, B_{0i}^*, B_2^*, B_3^*, B_4^*, B_5^*, B_6^*, B_7^*$.

The equation is solved at the number of pole pairs of the working winding $p_1 = 1$. The stator and rotor correspond to coefficients $L_{za}^* = 0.22$; $d_a^* = 0{,}6$ and $L_{zi}^* = 0.11$; $d_i^* = 0.6$.

The ratio of the radii of the average circles of yokes is $k_s = 0.475$. The length of the gap is $\delta^* = 50$.

To illustrate the fact of the absence of even harmonics with symmetric magnetization the figure 7 shows dependences $B_{2,3,4}^* = f(F_{0i}^*, B_1^*)$ at $F_{0a}^* = 8000$. The first quadrant corresponds to the consonant action of the MMFs of the control windings F_{0a}^* and F_{0i}^* with respect to the contour of the rotating field. Therefore, the even harmonics of the same name, generated respectively by the outer and inner yokes, coincide in phase, and the amplitudes of the resulting even harmonics have the greatest value. With a decrease in the MMF, F_{0i}^* the resulting even harmonics also decrease [3].

Since there are no even harmonics with symmetric magnetization, there is no "magnetic rectification" in the yokes [8]. Therefore, in the SM mode, the magnitudes of the constant magnetic inductions B_{0a}^* and B_{0i}^* take their natural values, determined respectively by the MMF F_{0a}^* and F_{0i}^*, the amplitude B_1^* and the magnetic state of the system.

The curves $B_{0a}^*, B_{0i}^* = f(F_{0i}^*, B_1^*)$ at $F_{0a}^* = 8000$ are shown on the figure 8. If $B_1^* = 0$ and $F_{0i}^* = var$, then the induction value $B_{0a}^* = 7.8$ remains constant, and the value B_{0i}^* changes, and the graph $B_{0i}^* = f(F_{0i}^*)$ is located in the 1st and 3rd quadrants symmetrically relative to the origin of the axes of coordinates. When $B_1^* > 0$ and $F_{0i}^* = var$ in the general case even harmonics appear in the field and "magnetic rectification" occurs in the yokes – these are additional constant induction components ΔB_{0a}^* and ΔB_{0i}^*, due to the imposition of even and odd saturation harmonics in them. With variations of B_1^* and F_{0i}^*, the saturation harmonics change, and hence the values ΔB_{0a}^* and ΔB_{0i}^*. Therefore, with a change in the MMF F_{0i}^* within $-8000 < F_{0i}^* \leq 10000$, the induction B_{0a}^* decreases with the transition from the 1st quadrant to the 2nd. When $F_{0i}^* = -8000$ there are no even harmonics in the field, and $\Delta B_{0a}^* = 0$.

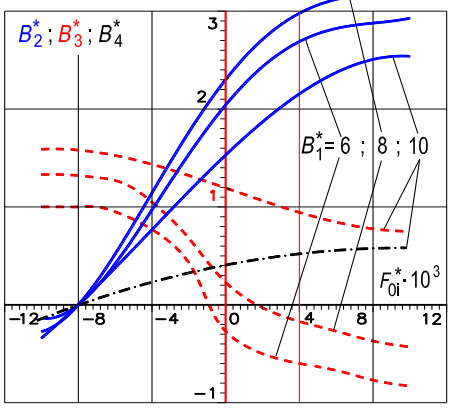

Figure 7. Dependence of the amplitudes of the 2nd, 3rd and 4th induction harmonics on the magnitude of the MMF F_{0i}^* at $F_{0a}^* = 8 \cdot 10^3$: B_2^* – solid lines; B_3^* – dotted; B_4^* – dash-dotted.

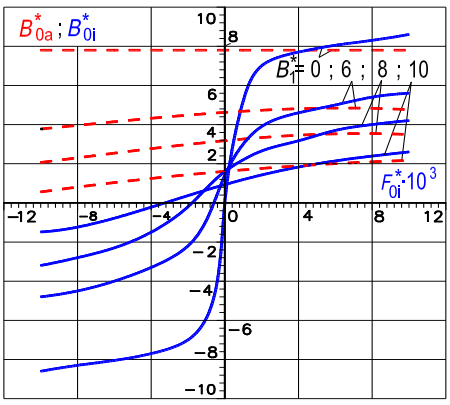

Figure 8. The dependence of induction values B_{0a}^* and B_{0i}^* on the magnitude of the MMF F_{0i}^* at $F_{0a}^* = 8 \cdot 10^3$: B_{0i}^* – solid lines; B_{0a}^* – dash-dotted.

For the values of MMF $|F_{0i}^*| > 8000$ (2nd quadrant) the phase of the resulting even harmonics and the sign ΔB_{0a}^* change to opposite ones. As for the $B_{0i}^* = f(F_{0i}^*, B_1^* \neq 0)$ curves at $F_{0a}^* = 8000$, their symmetry relative to the origin becomes broken due to the "magnetic rectification". When MMF

$F_{0i}^* = 0$, the presence of a constant induction in the inner yoke is determined only by "magnetic rectification", $B_{0i}^* = \Delta B_{0i}^*$. In order to avoid a constant induction in the inner yoke, it is necessary to apply some negative value of the MMF F_{0i}^*. For example, for $B_1^* = 8$ and $F_{0a}^* = 8000$ the induction $B_{0i}^* = 0$, if $F_{0i}^* = -1750$. The difference between the induction B_{0i}^* at $B_1^* = const$, $F_{0i}^* = F_{0a}^* = 8000$ and $F_{0i}^* = -F_{0a}^* = -8000$ is caused by "magnetic rectification".

An interesting fact is that the symmetric magnetization mode affects the 3rd harmonic of magnetic induction qualitatively the same as the mode of free magnetization by the 2nd harmonic (figure 5 and 9). In [3], experimental analogs of the calculated dependences shown in figure 9*b*.

Dependencies $B_{0a}^*, B_{0i}^* = f(F_{0a}^* = |-F_{0i}^*|, B_1^*)$ in SM mode, when $F_{0a}^* = |-F_{0i}^*|$, and in FM mode, are shown in figure 10. Curves must be used when calculating the loss in steel. As follows from figure 10, induction B_{0a}^* and B_{0i}^* in the SM mode are always less than those in the FM mode. Therefore, the yoke losses in the SM mode will be less than in the FM mode.

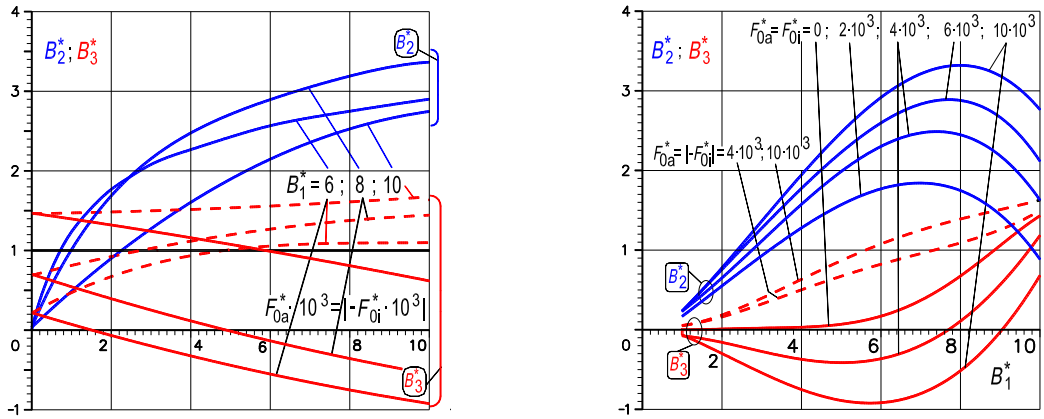

a *b*

Figure 9. The dependence of the amplitudes of the 2nd and 3rd harmonics in FM mode – solid lines; SM mode – dotted: *a* – on of MMF control windings; *b* – on of the induction amplitude B_1^*.

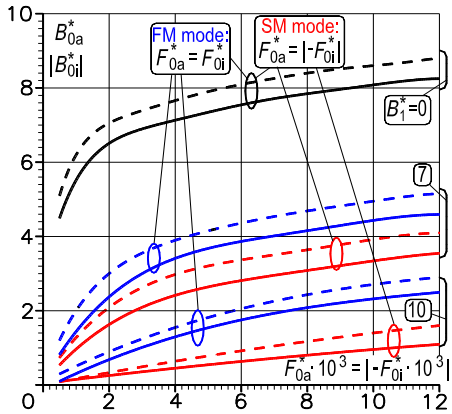

Figure 10. The dependence of the induction values B_{0a}^* and B_{0i}^* on the magnitude of the MMF control windings in the FM and SM modes: B_{0a}^* – solid lines; B_{0i}^* – dotted.

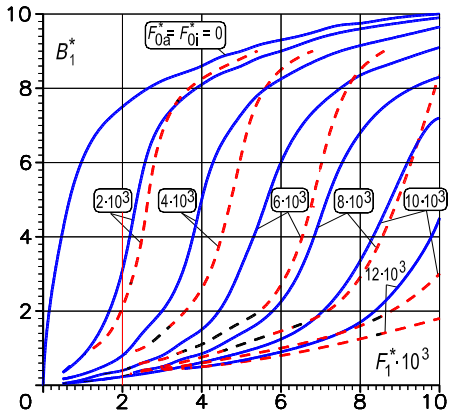

Figure 11. Dependence of amplitude B_1^* 1st harmonic of induction on amplitude F_1^* MMF: in FM mode – solid lines, $F_{0a}^* = F_{0i}^*$; in SM mode – dotted, $F_{0a}^* = |-F_{0i}^*|$.

The dependencies $B_1^* = f(F_1^*, F_{0a}^* = |-F_{0i}^*|)$, illustrating the increase in the range of current control in the SM mode, are shown on the figure 11. These graphs used in calculation of the reactor.

The mode of SM favorably differs from the mode of FM by elimination of the "shaking" vibrations, by the extended control range of the operating current, reduced losses in steel, enhanced stabilizing effect over current and increased speed, which is confirmed by the calculation and experiment [3].

The photo (figure 12) shows a prototype of a reactor, which was used study of the dependence spectrum of the induction of a rotating field in forced and symmetric magnetization modes on the amplitude of the first harmonic of field and control windings.

The photograph (figure 13) shows reactor with symmetrical magnetization, intended for use as a regulating element of the plasmatron power source air plasma cutting of metals [3].

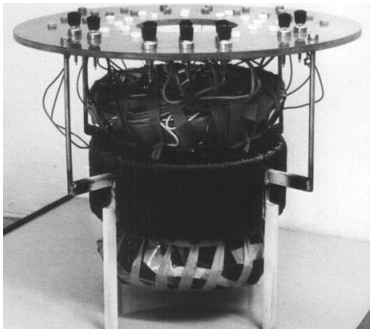

Figure 12. Reactor designed to study the field spectrum and magnetization modes.

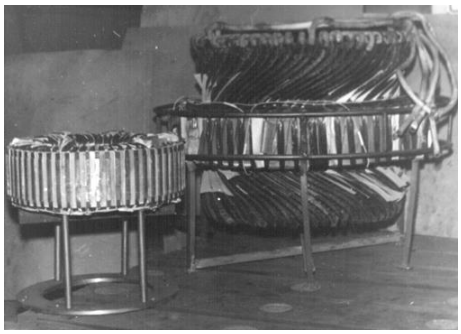

Figure 13. Reactor is made of stator plates of the stator from the engine VAO14-4.

Conclusions

- It is shown that the optimal, in terms of maximum current gain, is a reactor in the symmetric magnetization mode, which has a three-phase 2-pole working winding and transverse geometry of the magnetic circuit, corresponding to the stator plates of standard 4-pole AC electrical machines.
- It was found that the reactor in the symmetric magnetization mode favorably distinguishes the following qualities: increased control range of reactive power, enhanced stabilizing effect on current, reduced steel losses, increased speed and the absence of "shaking" vibrations of the magnetic circuit.

References

[1] Alexandrov G N 2002 Fast controllable reactor of transformer type 420 kV, 50 MV *Electrical Technology Russia* **3**
[2] Belyayev A N, Evdokunin G A, Smolovik S V and Chudnyi V S 2009 Use controlled transverse compensation devices in 500 kV transit transmission lines *Electrical Technology Russia* **2** pp 2-13 URL: https://elibrary.ru/item.asp?id=11700350
[3] Zabudskiy E I 2003 Combined adjustable electromagnetic reactors (Moscow: Publishing House Energoatomizdat) p 436
[4] Bryantsev A M 2003 Power reactors controlled by bias magnetization – as an element of the electroenergy system *Electrical Technology Russia* **1**
[5] Dolgopolov A G 2014 Controlled shunt reactors. The principle of operation, construction, relay protection and automation (Moscow: Publishing House Energia) 120 p
[6] Bryantsev A M, Makletsova E E *et al* 2003 Shunting reactors controlled by bias magnetization for (35-500)-kV grids *Electrical Technology Russia* **74(1)** pp 4-12
[7] Dolgopolov A G, Sokolov S E 2012 Controlled reactors. Technology review *Electrical Engineering News* **75(3)**
[8] Zabudskiy E I 2018 Mathematical modeling of controlled electromagnetic reactors (Moscow: Publishing House Megapolis) p 356
[9] Bengtsson C, Gajic Z, Khorami M 2012 Dynamic compensation of reactive power by variable shunt reactors: Control strategies and algorithms *CIGRE 2012* **C1-303**
[10] Zabudskiy E I 2016 Magnetization modes of controlled electro-magnetic reactors *Proc. XVI Int. Conf. on Electromechanics, Electrotechnology, Electromaterials and Components* (Moscow, Russia) pp 171–172

Acknowledgments

The publication has been prepared with the support of the "RUDN University Program 5-100".

Authors' background

Name	*Prefix*	*Research Field*	*E-mail*	*Personal web-site*
Zabudskiy E I	Full Professor	adjustable electromagnetic facilities for electrical power engineering control systems; mathematical modelling of facilities "anatomy" and "physiology" based on Maxwell's field theory, theory of nonlinear circuits and computer technologies; microprocessor systems for electrical power engineering controlled reactor, rotating field, cross-sectional magnetic circuit, forced magnetization, free magnetization, symmetrical magnetization	zabudskiy-ei@rudn.ru	http://zabudsky.ru
Balandina G I	Associate Professor	control system synthesis, energy facilities automatic control systems, genetic algorithms	balandina-gi@rudn.ru	-